Modelling and safety assessment of observed sliding damage in a masonry rib vault

Grigor Angjeliu[1*], Giuliana Cardani[1], Dario Coronelli[1], Thomas Boothby[2]

1) Department of Civil and Environmental Engineering, Politecnico di Milano, Italy
2) Department of Architectural Engineering, Pennsylvania State University, USA

* Corresponding Author (grigor.angjeliu@polimi.it)

Abstract *(limit 250 words)*

Frequently observed damage in historic masonry vaults has always given rise to concerns on their stability. The effect of present damage on masonry vaults structural response should be taken into consideration during structural analysis as it clearly affects its behavior.

The aim is to propose a method to study the safety of vaults, setting up a finite element model with a limited number of discontinuities, based on the consideration of the vault construction and damage observation.

A case study from Milan cathedral is adopted where damage is documented. A complex damage mechanism characterized by sliding of voussoirs and detachment of the rib from the web was documented in the 1960s. The results show the possibility to analyze the evolution of the observed mechanism and to evaluate numerically its safety in function of the documented settlements.

Technical applications of the present work include interpretations of the causes of observed damage, estimation of the level of settlements based on observed damage, and numerical evaluation of the safety of the current mechanical state.

Keywords: Damage modelling, Observed damage, Safety assessment, Masonry, Rib Vaults.

1 Introduction

Documentation and interpretation of the crack pattern is a common practice in historic buildings [1]. In a historic construction, not all the observed cracks are detrimental since several structures can also crack in service conditions [2]. Masonry, being a material with little or no tensile strength is even more susceptible to cracking. Among structural members, the most vulnerable to cracking are masonry vaults, since positioned at the top of the construction, where all the induced displacements are magnified as compared to the base (either from soil settlements or seismic actions).

The structural assessment of historic masonry vaults has been carried out employing three main approaches: Limit Analysis, Finite Element Method and Discrete Element Method [3]. Limit analysis has seen considerable improvement since its first development by Heyman [4]. Later versions include applications that take into account structures' three-dimensional configuration [5], or seismic loading [6]. The sliding resistance and interlocking of blocks have been demonstrated to be critical in the structural response [7, 8]. Continuum Finite Element Models on the other hand are very common for the analysis of historic structures [9]. Close to collapse, diffused cracking and excessively deformations result in convergence problems and interruption of the analysis. In this case the discontinuum finite element models (where discontinuities are introduced using interface elements) [3, 10, 11] or discrete element models [12] are more suitable, as they can simulate separation of parts, and thus better approximate the real failure of masonry structures.

Considering current technological levels, the analysis of masonry vaults should consider the three-dimensional configuration [13]. Structural models of masonry vaults must be created staring from point-cloud measurement and should include the main members: tas-de-charge, arch, rib, web, crown and rubble-fill [14]. This in aligned with recent research which suggest an integrated approach between advanced numerical models, modern survey and detailed geometry [15]. Part of this is also the structural damage, which could be considered as an input in the analysis process. Depending on the type, scale and intensity, structural damage can reduce and influence the capacity of masonry members. Moreover, under constant loads and continuous actions it can also further develop [16]. Among the most peculiar types of damage [17], are the sliding cracks (Figure 1), typically observed in the arches and ribs which are not considered in the traditional Heyman models [4].

Figure 1. Reims Cathedral, France: Example of shear sliding indicated with dashed rectangle.

The possibility of introducing the observed damage in the structural analysis has found some application. Among the most diffused in the current practice is the analysis of collapse mechanisms, where the observed crack pattern is used to pre-select a mechanism among all the possible ones [18]. The possibility of introducing the observed damage in finite element simulation is less frequent. The peculiar crack system affecting the Dome Santa Maria del Fiore was considered, by updating the FE model with new unilateral contact elements along the areas where non-admissible tensile stresses arises [19]. Other applications are noted on reinforced concrete structures. Talley et al. [20] studied pre-damaged scaled models of concrete column. The capacity of the pre-damaged elements was evaluated experimentally and numerically using the ATENA finite element software. Recently, Blomfors et al. [2] studied a methodology to incorporate pre-existing cracks into finite (FE) analysis for improved structural assessments. Two different approaches were investigated: (1) weakening the continuum elements at the position of a crack and (2) introducing contact elements with weakened properties.

In this paper the structural response of the vaulting system is studied. The objective is to integrate the surveyed damage in the three-dimensional model, with the aim of understanding the entirety of the observed damage and estimating possible damage threshold.

The structural geometry is created based on a parametric model developed in previous research [21]. The here proposed includes only interfaces between structural members, related to the vault construction (e.g. web and arch or web and rib) [21] and where important cracks are observed. We have adopted a much simpler model than would be required for an all-inclusive model with an elevated number of interfaces that were meant to investigate every possible mode of failure [22, 23]. This enables the possibility to deepen the knowledge on the observed damage, and to use it as a starting point in the analysis process, and to use it as a starting point in the analysis process.

2 Vaults and case study

2.1. *Historical notes on ribbed vaults construction*

The role of the ribs in vaults from the structural point of view has always been a source of debate among experts in the field of historical structures [24, 25]. Specifically, focusing on the rib sliding mechanism, it is important to highlight that the role of the ribs in cross vaults is worthy of specific investigation, since the techniques adopted from time to time to solve the problem of covering large spans can differ. One way of understanding the construction technique of a masonry vault, when it is not possible to carry out direct inspections or non-destructive investigations, is to base it on the observation of the damage present. Great help can also be provided by historical archives, which can provide reports, descriptions, drawings and photos of past interventions [26].

With reference to the construction of masonry vaults, the Romanesque builders first constructed perimeter arches (head arches) and diagonal ribs and then added webs [27-31]. This idea was crucial for the development of Gothic structures and ribs in cross vaults which were then employed as permanent frames for building the webs, thereby saving on large heavy wooden centering. Porter also wrote that ribbed vaults were easier, or less expensive than others to build. This, in fact, was the case for ribbed vaults, which may be constructed with the aid of a very light timber centering, whereas a groin or barrel vault requires a heavy centering [30].

Regarding ribs geometry, it was found that the elliptical shape was not convenient for the meeting of the joints since the key lines remained horizontal. It was necessary to arrive naturally at the pointed arch and then at the raising of the vault key to increase their stability (also allowing for larger spans to be covered). Therefore, the semicircular shape was preferred for the diagonal arches. This was particularly important in the case of stellar vaults with the load-bearing ribs, where the sails are simple and as light as possible [27]. This characterized the medieval style and particularly the Gothic, with diagonal ribs protruding from the intrados of the vault.

Finally, different solutions can be used to join ribs and webs: webs either embedded in the sides of the specially shaped ribs or resting on top, forming a groin vault above (Figure 2). In this last case, the vault is continuous and is supported on the ribs, displaying a load carrying function: if the rib fails, the web can resume the load bearing capacity. In the former case, the rib works as a shear connector and the integrity of the web depends on the rib [32].

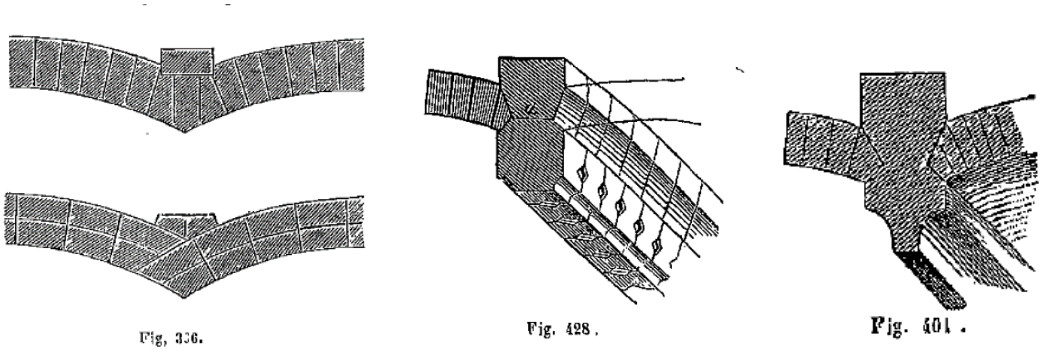

a) b) c)

Figure 2. a) Section of the edges (intersection between webs) of a groin vault; b) section of a rib with interlocking webs in a stone rib vault with a stem [27].

2.2. *Case study: A quadripartite vault in Milan Cathedral*

A quadripartite vault in Milan Cathedral, where rib sliding was document in 1965, is adopted as a case study for the development of the methodological approach. The damage documented in vault 113 of the Cathedral of Milan included a sliding of the rib voussoirs, accompanied by 97 mm detachment of the rib from the web (Figure 3a, b). The vault is located in the first bay of the deambulatory, adjacent to the south transept (Figure 3c). The vault typology is consistent with other vaults located in the aisle and in the ambulatory part of the cathedral. The damage was repaired in the subsequent years by correcting the rib deformation and replacing the damaged voussoirs [33].

A recent survey carried out by the authors in the same vault, showed some signs of damage in the voussoirs. It was interesting to note the distorted arch in the transversal direction of the same vault (Figure 4a). Ferrari da Passano [33] states that in this arch difficult structural consolidation works have been carried out, similarly to those for the rib of the same vault.

The survey was extended further in direction of the apse, focusing on the vault 119, which is symmetric to the vault 113 with respect to the cathedral East – West axis, hence in similar structural conditions (Figure 3c). Damage was observed again on the transversal arch (Figure 4b). The upper part of the arch was confined within a steel cage.

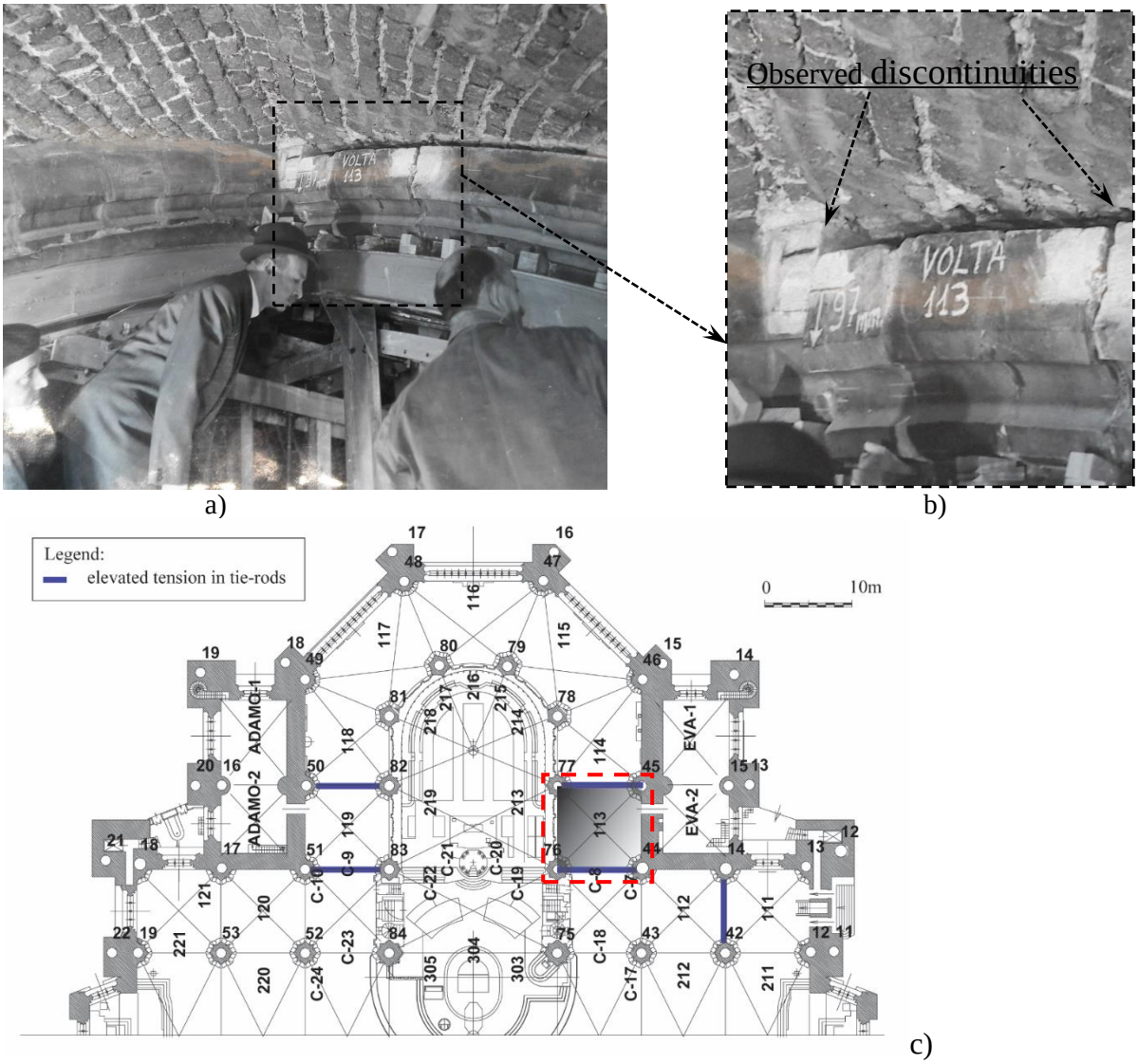

a) b) c)

Figure 3. Milan Cathedral, circa 1965: a) Sliding mechanisms in the vault 113, b) detail, c) Location of the vault object of study. *Courtesy of the Veneranda Fabbrica del Duomo di Milano*.

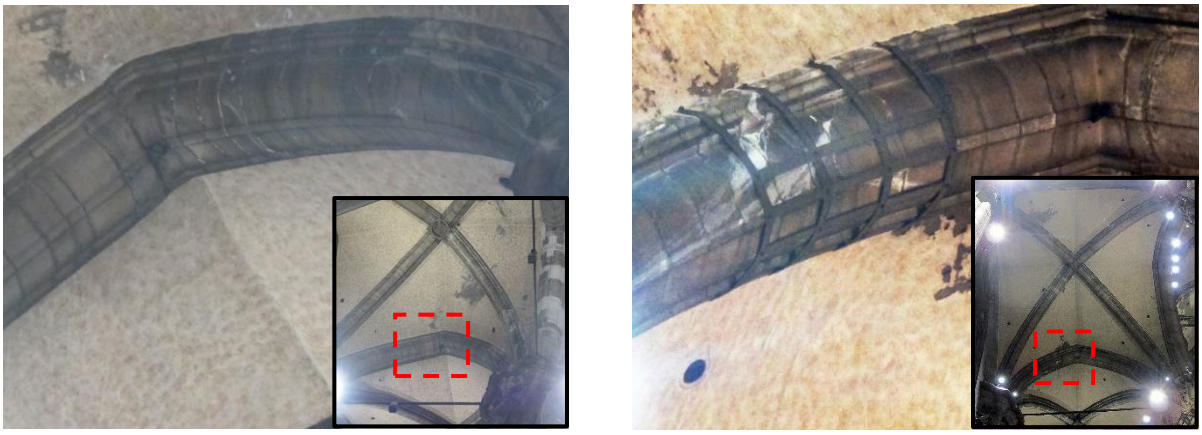

Figure 4. a) Distorted arch observed in the vault 113, b) Strengthening observed today in the vault 119, symmetrical to vault 113 with respect to the cathedral longitudinal axis.

Investigation into the causes of the described damage revealed that the lowering of the water table by 25 m in the first half of the 20th century, caused subsidence settlements with redistribution of internal forces, hence heavy damage [33-36]. Traces of past damage can still be noted today in the cathedral [37]. The data of the actual monitoring system in the Cathedral of Milan since 1965 were studied and is concluded that most of the soil settlements were observed before 1965, after the damage was observed in the cathedral. Furthermore, experimental studies, which have determined elevated levels of stress in the tie rods [38], provide further evidence about settlement of the supports. Finally, detailed studies of Angjeliu et al. [39, 40], demonstrate numerically a clear correlation of the effect of settlements on the elevation tension force in the iron ties measured by Vasic [38].

2.3. *Geometry*

The dimensions in plan of the vault are 9.6m x 9.6m (Figure 3c). The pointed arches are made of stone voussoirs and the cross-section depth is 0.57 m, while for the rib the cross-section depth is 0.52 m. The web is made of brick masonry, 0.38m thick.

With regards to the connection between ribs and webs, no precise indication is given other than the drawing reported by Ferrari da Passano [33], with measurements only of the intrados (Figure 5). For the extrados, an extract from the archives annals of the Cathedral, seems to affirm that the shape of the rib stones does not allow the interlocking with the brick vaults [archives annals January 21, 1409] [41]. These indications, together with the photo of the damage documented in the 60's by Ferrari da Passano (Figure 3), support the assertion that in the Duomo the brick masonry webs are lying above the stone ribs with a smooth extrados, without being embedded in the ribs.

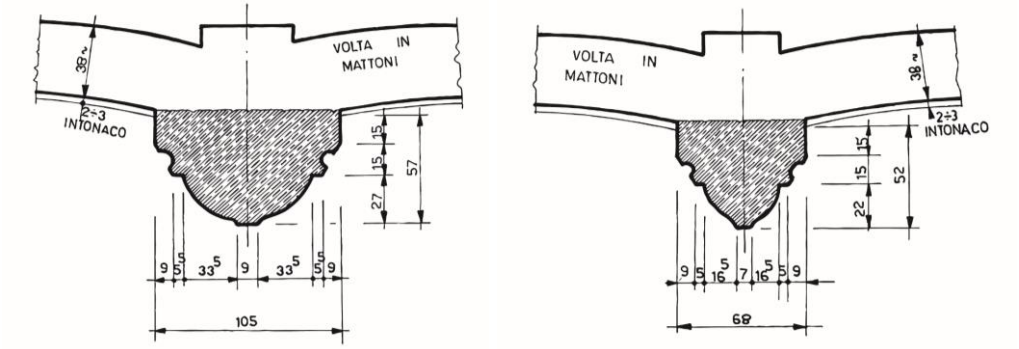

Figure 5. Cathedral of Milan. Detail of the connection in the vault, a) section of the head arch with webs and, b) section of the rib with webs. *Courtesy of the Veneranda Fabbrica del Duomo di Milano.*

3 Numerical modelling

3.1. *Model formulation*

The idea of starting from a damage state as observed in practice is investigated and elaborated in this section. To this aim, it is proposed a three-dimensional discontinuum finite element model with a limited number of interfaces (Figure 6a). This model represents a model with less interfaces compared to a common full discrete model [23].

The here proposed model (with a reduced number of interfaces) includes only interfaces between structural members and where important cracks are observed. A second model developed in a previous research [22], which includes a more extensive set of interfaces (Figure 6b) is used as a benchmark. Both models use the same complex 3D geometry, that includes all the structural parts of historic masonry vaults.

The hypothesis that the observed sliding and detachment mechanisms (documented in the middle of the 20th century) were caused by the soil settlements will be investigated in detail (see section 2.2). Therefore, the vault model is analyzed under gravity loading and settlement of one of the supports. The loading is considered step by step as the parts are added through a staged construction analysis.

The boundary conditions represent the connection of the vault with adjacent elements (walls or vaults). Side restraints Γ_x ($u_x=0$) and Γ_y ($u_y=0$) are used to confine the model such as to simulate the buttressing effect of adjacent walls or vaults (Figure 7). Vertical restraints Γ_z with normal in z-direction ($u_z=0$) simulate the column that supports the vertical reaction force.

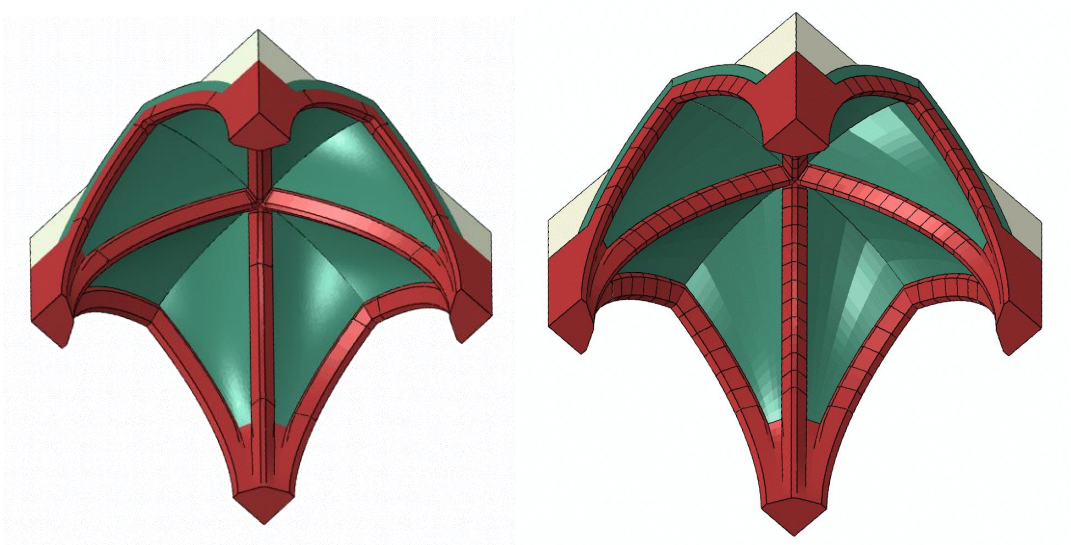

Figure 6. Contact based numerical models: a) Model with limited number of contacts (proposed in this work), b) Model with full number of contacts developed previously in [22, 23] *(printed with permission from Taylor & Francis*).

3.2. *Modelling discontinuities*

Discontinuities are introduced using contact elements, for which the constitutive model describes a direct relation with the stress vector and the relative displacement vector along the interface [10]. The solids feature a plasticity-based model and discretized with C3D8R finite element (see section 3.3), while the interfaces with a Column friction model (see section 3.4).

The vault model is subdivided into members with different mechanical properties, which are marked by different colors in Figure 6. Contacts are introduced between the structural members (web – rubble fill, web – arch, web – rib, web – web, web – tas-de-charge, and rubble-fill – tas-de-charge) and where damage is observed. The position of contact elements is reported in Figure 7. The insertion of contact between structural members is facilitated during the modelling phase given the fact that the geometry is generated using parametric procedures [21]. Hence, the deformations are concentrated mostly within the interfaces, but the blocks can also be deformed.

In relation to the present vault, one crack is inserted in the mid rib (Figure 6a, Figure 7) as observed (Figure 3b). Furthermore, in arches and ribs, two interface locations are inserted at the abutments and at the crown as observed frequently. The considered position of interfaces gives the possibility to simulate slipping of the voussoirs, detachment between members, and local compression phenomena at the corners of the voussoirs.

In the case of the models with a limited number of interfaces, the minimum number of contact elements with respect to a complete contact-based model will be defined by the number of interfaces required to simulate at least a possible collapse mechanism in each arch/rib. It is noted here that these models would also be more computationally affordable, since less contacts are employed.

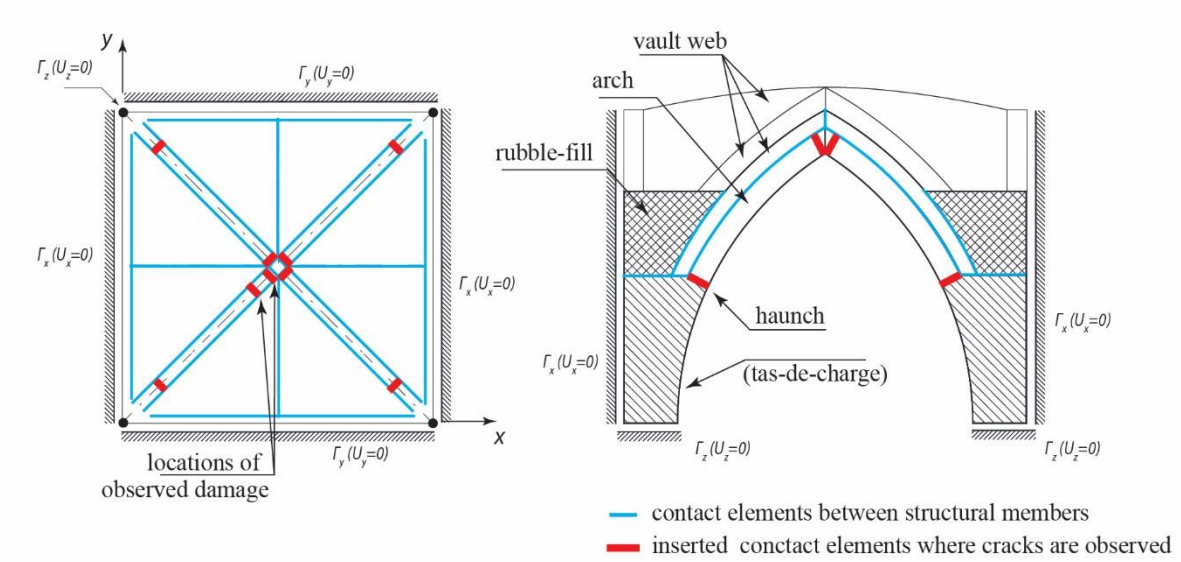

Figure 7. Schematic location of the contact elements: a) Projection in plan of the intrados view, b) elevation.

3.3. *Constitutive model for continuum*

The masonry is modelled with the so-called Concrete Damage Plasticity constitutive model which is already implemented in the Abaqus software [43]. A detailed description can be found in the Abaqus Manual [44]. The model has been used also by other authors for the study of masonry structures [45, 46]. In the following we give a brief description of the key features. The constitutive model considers plastic strains in tension and in compression with the following relations:

$$\sigma_t = E\left(\varepsilon_t - \varepsilon_{t,pl}\right) \tag{1}$$

$$\sigma_c = E\left(\varepsilon_c - \varepsilon_{c,pl}\right) \tag{2}$$

where:

σ_t (σ_c) – axial tensile (compressive) stress,
E – elastic modulus,
ε_t (ε_c) – total strain in tension (compression),
$\varepsilon_{t,pl}$ – equivalent plastic strain in tension,

$\varepsilon_{c,pl}$ – equivalent plastic strain in compression.

The yield surface is a modified Drucker-Prager surface with a smooth tip and a non-circular cross section in the space of the principal stresses. The model is based on a non-associated potential plastic flow defined by dilatation angle ψ, and the eccentricity ϵ. The parameter f_{b0}/f_{c0}, denotes the initial equi-biaxial compressive yield stress to initial uniaxial compressive yield stress; μ is the viscosity parameter used to improve numerical convergency, in the softening regime; K_c, is the ratio between the deviatoric stress in uniaxial tension and compression. The values for the parameter are summarized in Table 3.1.

Table 3.1. Constitutive model properties for masonry

Parameter	ψ	ϵ	f_{b0}/f_{c0}	K_c	μ
	36°	0.1	1.16	0.667	0.0002

The material model is characterized by the weight, γ, modulus of elasticity, E, Poisson's ratio ϑ and description of the tensile cracking and compressive crushing. The tensile behavior is defined as a stress displacement law, with a linear part up to the tensile strength, f_t. The softening is characterized by the fracture energy G_f^I which is used for mesh dependency regularization. The compressive strength values is defined with fc, and the law to model the compression part is the one proposed by Lourenco in [11], with the introduction of the fracture energy in compression G_{fci}, The adopted material properties are described in Table 3.2. The mechanical properties, are chosen based on the documented visual quality on site [39, 47] and based on some previous mechanical tests carried out in the 1960 – 1980 [33].

Table 3.2. Material properties

Structural elements	γ $\left[\frac{kN}{m^3}\right]$	E $\left[\frac{N}{mm^2}\right]$	ϑ $[-]$	f_c $\left[\frac{N}{mm^2}\right]$	f_t $\left[\frac{N}{mm^2}\right]$	G_f^I $\left[\frac{Nmm}{mm^2}\right]$	G_{fci} $\left[\frac{Nmm}{mm^2}\right]$
Brick masonry	20	2000	0.2	5	0.20	0.012	1.2
Stone masonry (voussoir)	22	8000	0.2	10	1.00	0.02	1.5
Fill	16	800	0.2	2	0.15	0.010	0.5

3.4. *Constitutive model for contacts*

The contact elements are positioned at the interface between solids. In the normal direction a hard formulation contact is enforced through the direct method, while the tangential behavior is analyzed by a Coulomb friction model. The description follows the implementation in Abaqus [44]. It assumes that no relative motion occurs if the equivalent frictional stress is less than the critical stress:

$$\tau_{eq} = \sqrt{\tau_1^2 + \tau_2^2} < \tau_{crit} \tag{3}$$

The critical stress is defined as:

$$\tau_{crit} = \min(\mu p,\ \tau_{max}) \tag{4}$$

where:
μ – friction coefficient
p – contact pressure
τ_{max} – specified critical value

Slip can occur if $\tau_{eq} = \tau_{crit}$. In the current simulations a value of $\mu = 0.6$ is chosen.

4 Results

The contact-based model with a limited number of interfaces is used in this section to investigate the ribbed vault failure up to collapse. The objective is to set the base for a procedure to quantify the level of settlements that have taken place and the safety level, based on the observed mechanism.

4.1. *Correlation of observed slip-plane with settlements*

Based on the numerical results a relationship between, the displacement at the observed shear slip plane and the vertical settlement of one of the supports is proposed to be used in order to investigate the system state as a function of the settlements (Figure 8).

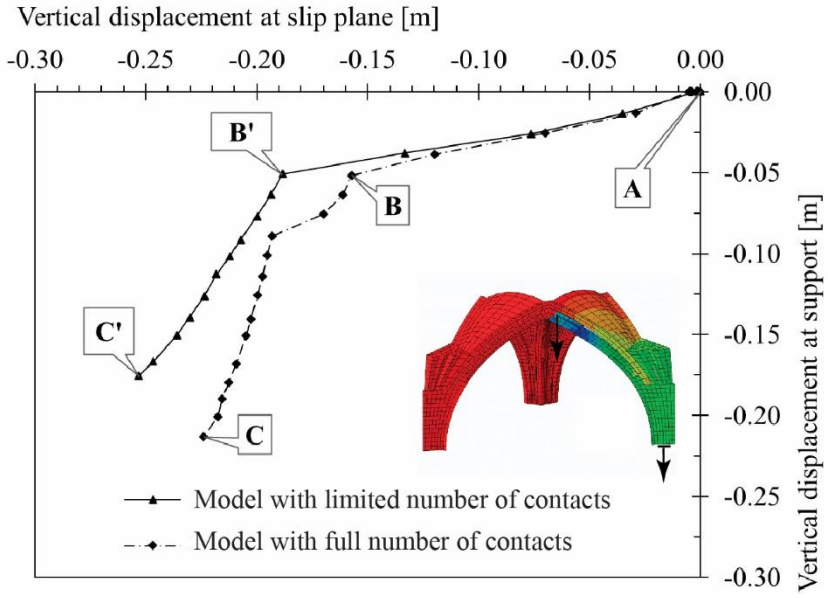

Figure 8. Numerical correlation of slip plane displacement with support settlement.

The graphs are obtained from two different discontinuum finite element models: a) Model with limited number of contacts, and b) Model with full number of contacts. In the horizontal axis, the vertical displacement at the slip plane is plotted and in the vertical axis the vertical displacement at one of the supports is shown. The results show that the displacement fields

are quite close between each other (figure 8). Hence, using a lower number of interfaces provides a suitable accuracy for the object of the study.

Focusing on the comparison of the collapse kinematics, the FE model with full number of contacts shows a similar response compared to the model with fewer contacts. The model with less contact elements successfully predicted the observed damage, with sliding of the voussoir and detachment of the rib from the web. Therefore we can conclude that in comparison to the FE model with full number of contacts, the present model with less contacts is computationally more efficient, without a particular reduction of the predictive capabilities (compare Figure 9a with Figure 9b).

During modelling with the present approach beside the successful simulation of the rib mechanism, it was also possible to simulate the observed damage in the transversal arch (Figure 4). This further corroborates the hypothesis of the support of support settlement.

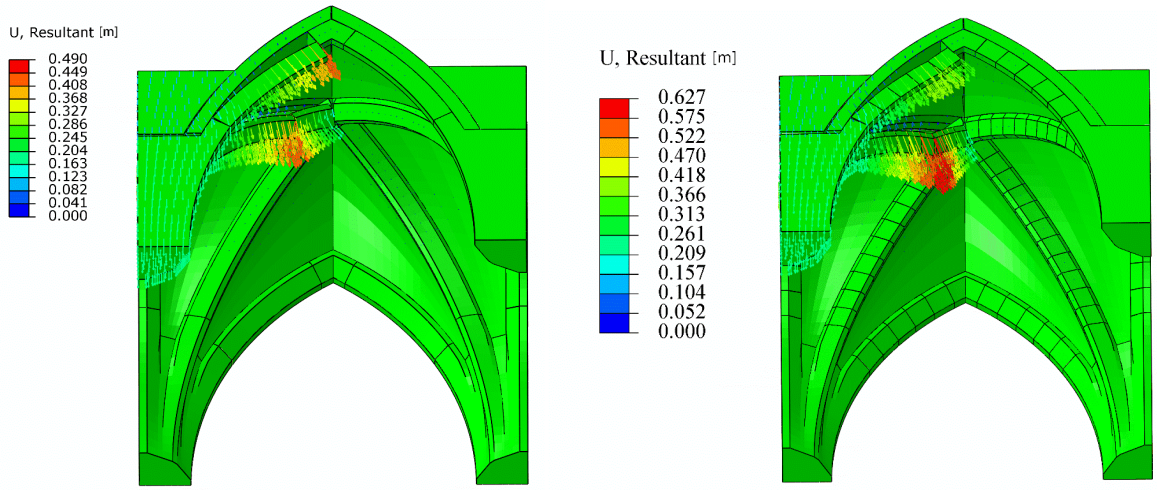

Figure 9. Kinematics at collapse simulated with the FE model with: a) present model with limited number of contacts and b) model with full number of contact elements (ri-elaborated after [22]).

4.2. *Interpretation of the collapse mechanism through the capacity curve*

Referring to the capacity curve plotted in Figure 8, we can define two parts based on the structural system response to settlements.

Part A – B: Small differential settlement in the order of millimeters is enough to cause damage to the system. The plastic strains develop mainly in the web. At this point, close to the boss a sliding mechanism develops in the connection with the rib. The numerical analysis shows the onset of this phenomenon even under self-weight, while differential settlements have a marked effect on the further development of voussoir sliding. The damage mechanism is associated also with a detachment of the web from the rib.

The mechanical state in the part A – B can be called a service state, as the progress of this mechanism will not lead the structure to collapse. The computations show the sliding mechanism evolves up to a 50mm settlement, when the sliding is blocked as the contact pressure increases with progression of settlements (Figure 8). The same trend is confirmed also by the model with full number of contacts (Figure 9). In Figure 8, this part is shown by the linear part of the graph.

Part B – C: The arrest of the sliding mechanism is followed by a new bending mechanism. The computations show that the evolution of this mechanism will bring the rib to collapse. In the Figure 8, this is shown by the approximately vertical part of the graph. It shows that the sliding mechanisms is in a stable state, and this bending mechanism is governing the behavior of the system up to the collapse.

4.3. *Safety assessment of the observed damage and settlement prediction*

The safety evaluation is based on the correlation between the support settlements and the observed rib – web detachment. If the detachment is known from the visual observations in-situ, it is an indicator of the current system state. Therefore, was used to locate the current system state on the graph in Figure 8. In the case of the vault analyzed in the Cathedral of Milan, the observed displacement of the rib voussoir relative to the web is 97 mm (Figure 3), therefore, the estimated level of settlement can be calculated as approximately 30 mm using the developed graphs (see blue line in Figure 10). The estimated value is a meaningful soil settlement. This level of soil settlement or even higher levels were measured during the 1965 survey in the Cathedral of Milan by the team led by Ferrari da Passano [33].

The first part A – B is a linear branch, and apparently does not present a hazard, while the part B – C can bring the system to collapse. Therefore, point B limits the displacement capacity of the system in a service state. This can be named as an unstable state of the system.

$$d_{sp\_y} = 157\ mm$$

$$d_{sp} = 97\ mm$$

The system state, with a measured slip plane displacement of 97 mm, is at 62 % (97/157 mm) to the limit of the displacement capacity. The displacement safety factor SF can be calculated as:

$$\mathrm{SF} = \frac{d_{sp\_y}}{d_{sp}} = \frac{157\ mm}{97\ mm} = 1.62$$

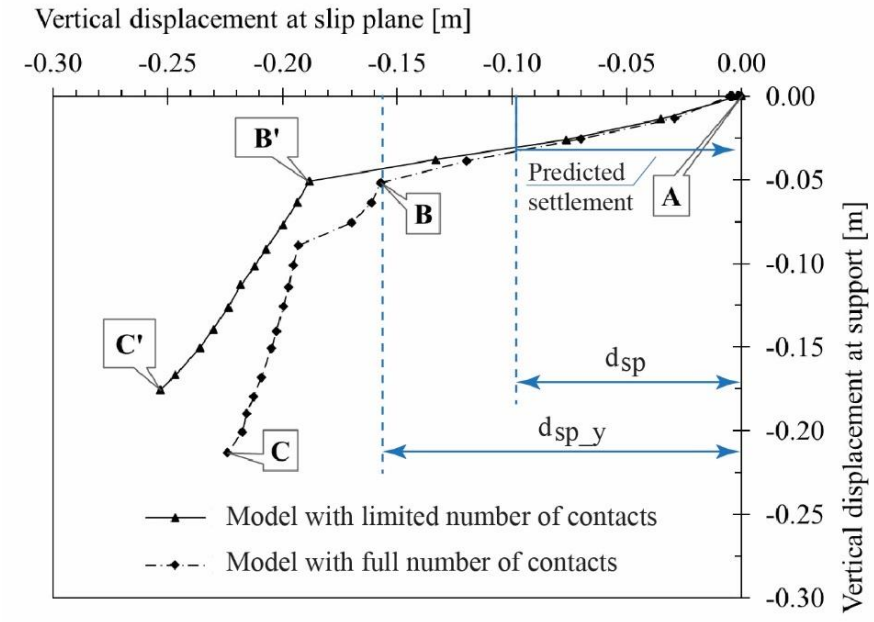

Figure 10. Safety assessment and settlement prediction through the proposed capacity curve.

5 Discussion

This study addresses the application of the discontinuum finite element analysis to the study of damage in vaulted structures. The reader is referred to previous work in [42], where the finite element discontinuum analysis has been validated on a barrel vault scaled model tested under differential settlements. The objective of the present work is to address the application in large scale problems. In particular, the setup of an efficient modelling strategy was developed, based on a reduced use of contact elements and an innovative procedure for the safety assessment in real applications proposed. Starting from visual observations and records of the history of this building, we developed a less extensive model, aimed for the investigation of a specific observed failure mode.

In the present FE model with a limited number of contacts, the new failure modes (beside those oriented by the introduced damage) are slightly more difficult to spot because of the lower number of interfaces. However, the development of plastic strains in an element can successfully be used to spot these phenomena and new interfaces can be introduced at a later stage.

This method could be employed for the investigation of any other specific failure mode and be used as a preliminary monitoring system. Furthermore, it is noted that the present developed models require less and less computational power than a model with full number of contacts, thus becoming more available to the practitioner (simulation time is estimated at 2 hours against up to 24 hours for the simulations considering full number of contacts).

From a methodological point of view, similar relationships to the ones created in Figure 10, can be created between other parameters, depending on the visual inspected mechanism in situ, e.g., the magnitude of opened cracks at the vault crown line due to settlements. Therefore, the numerical model, is used to create relationships between experimental observations and certain causes (or inputs of the numerical model) such as settlements, temperature, etc. In return, the created relationships can be used to evaluate the state of certain observed phenomena.

The relative proportions of the elements are obviously relevant. In some cases, the ribs can be so slender as to become merely decorative. The phenomena discussed here correspond to systems where the relative proportions of rib and vault are such that each element can be considered to bear a sizeable part of the load.

According to the construction scheme the structural response can be expected to change, as well as the suitable models. Simple “slicing” techniques [4, 48] are based on the assumption of portions of the web bearing as arches directly on the ribs. The web detached from the rib acts as a shell, thus making these schemes too simple for the analysis of the vault.

The “no sliding” assumption proposed by Heyman [4] does not correspond to the observations and mechanisms studied here. Figure 11 describes the classical mechanism analysis of the vault rib with sliding included. In the first part of the figure, a primary mechanism includes sliding at a joint near the crown of the arch (A), induced by vertical support settlement (B). Increase of shear resistance in the sliding joint (A) due to higher contact pressure with progression of settlement causes the sliding to be self-limiting. This induces a secondary mechanism that includes support settlement (B), an intrados hinge at the sliding joint (C) and at the support (D) and an extrados hinge (E) closer to the crown than to the support. The existence of these

settlement, sliding, and hinge points has been confirmed by the analysis in the foregoing exposition.

The rib mechanism shows a combination of sliding and rotation in a sequence, with the sliding taking a leading role initially (Figure 11a). The following flexural mechanism corresponds to a classical three hinge scheme in the rib, accompanying the support vertical settlement (Figure 11b).

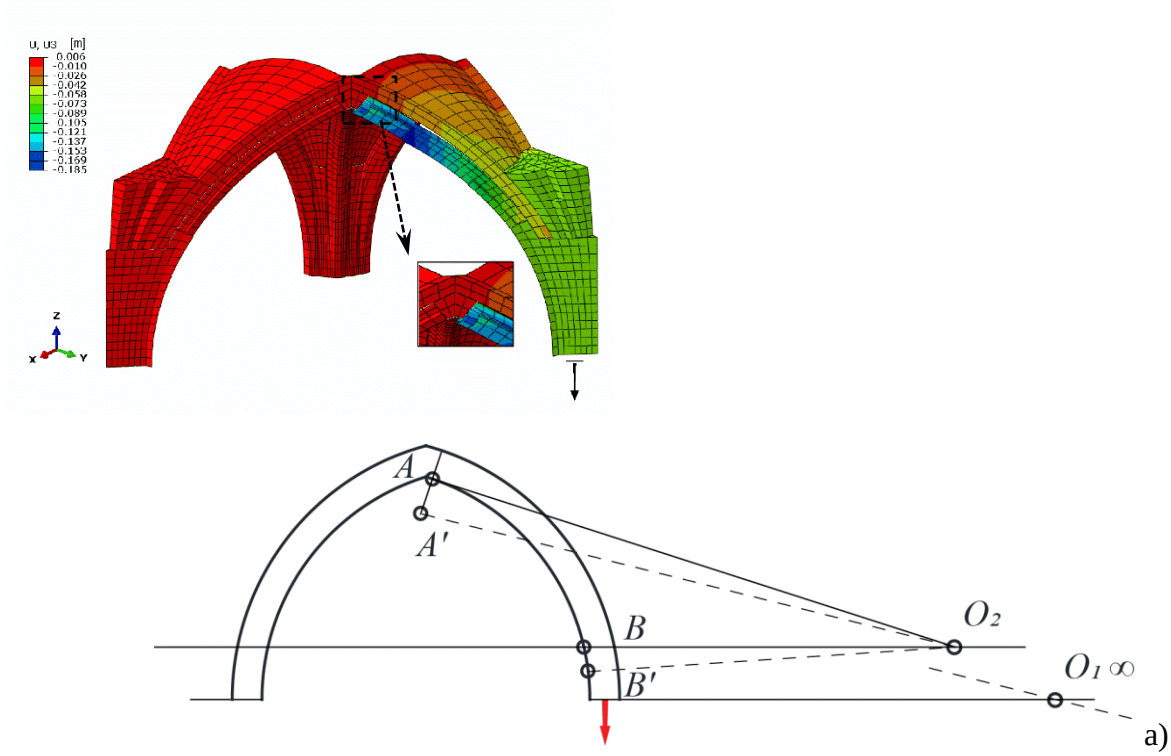

a)

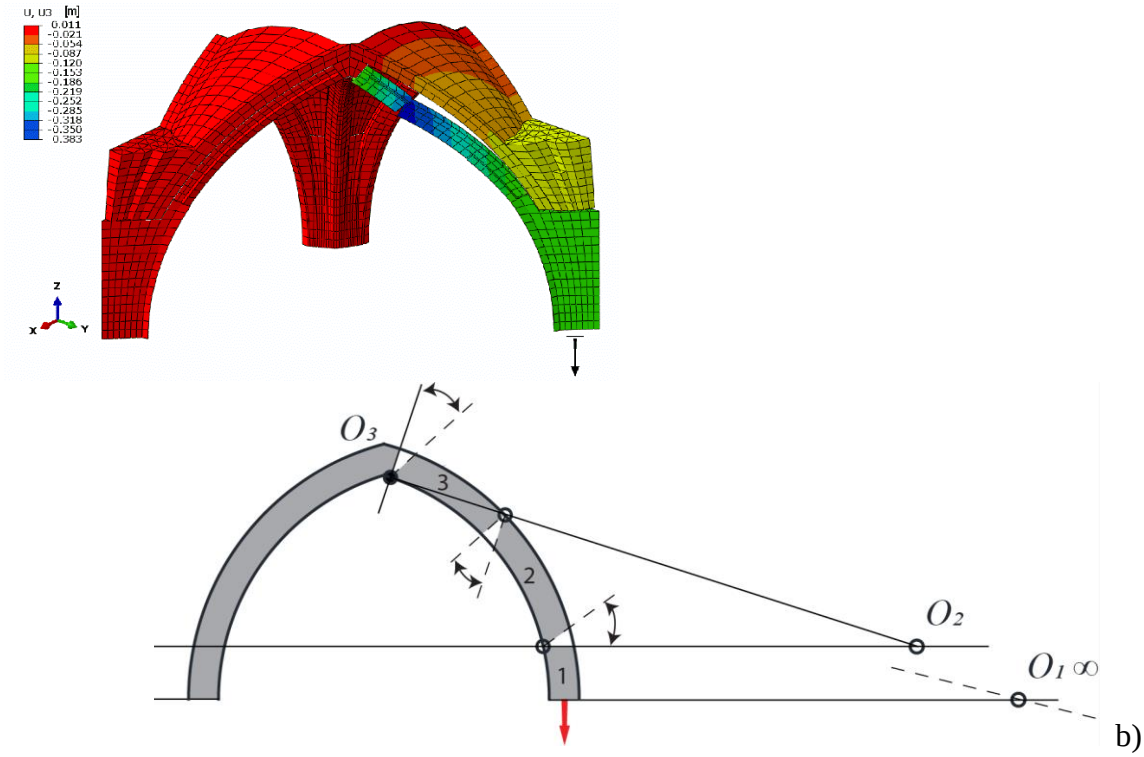

b)

Figure 11. Classical mechanisms analysis: a) primary mechanism related to sliding, b) secondary mechanism with hinging.

6 Conclusions

In this paper the structural response of historical masonry integrated with observed damage, is investigated through accurate numerical FE models with contacts. Here the study of the structural response of the square vaults of Milan cathedral is adopted. The application of the detailed three-dimensional models was proved to be essential for the simulation of the complex collapse mechanism of masonry vaulted structures. The increase of sophistication produces results useful in the correlation between inputs and damage observations.

The observed damage is successfully integrated in the numerical FE model by introducing a limited number of contact elements, but with a marked reduction of the computational time compared to the model with the full number of contacts. In this case the introduction of damage is essential for orientating the modelling results.

The clear relationship developed between observed damage mechanism and settlements, allowed the creation of a mathematical correlation between the voussoir sliding and settlement in one of the supports. A curve, support-settlement and observed voussoir-slip was computed, giving rise to a novel procedure in evaluating the practical safety of the collapse of this mechanism or in estimating a possible settlement based on the measured slip plane. This strategy is general and can be applied similarly to other vaults, or structures. In the present case based on the observed 97 mm of sliding, a 30 mm of support settlement can be predicted, that is a range of settlements measured in Milan Cathedral. The observed mechanism is judged here to have reached 62% of its displacement capacity, hence a safety factor of 1.62.

Technical applications of this study include interpretations of the causes of observed damage, study of preventive and planned maintenance works such as the replacement of the voussoir and numerical evaluation of the safety of the current observed state.

Acknowledgements

The authors are grateful to the ‘‘Veneranda Fabbrica del Duomo di Milano”, for making it possible to work in the Cathedral of Milan, within the 2015–2018 Agreement with the Politecnico di Milano coordinated by Prof. Stefano Della Torre and Ing. Francesco Canali.

References

[1] P. Beckmann, Structural analysis and recording of ancient buildings, in: Symposium on structures in historic buildings. Provisional papers. Rome, 14-18 sept. 1977, Iccrom, 1977, pp. 8.

[2] M. Blomfors, C. G. Berrocal, K. Lundgren, K. Zandi, Incorporation of pre-existing cracks in finite element analyses of reinforced concrete beams without transverse reinforcement, Engineering Structures, 229 (2021) 111601.

[3] P. Roca, M. Cervera, G. Gariup, L. Pela’, Structural Analysis of Masonry Historical Constructions. Classical and Advanced Approaches, Archives of Computational Methods in Engineering, 17 (2010) 299-325.

[4] J. Heyman, The stone skeleton, International Journal of solids and structures, 2 (1966) 249-279.

[5] P. Block, L. Lachauer, Three-Dimensional (3D) Equilibrium Analysis of Gothic Masonry Vaults, International Journal of Architectural Heritage, 8 (2013) 312-335.

[6] N.A. Nodargi, P. Bisegna, A finite difference method for the static limit analysis of masonry domes under seismic loads, Meccanica, 57 (2022) 121-141.

[7] E. Mousavian, C. Casapulla, The role of different sliding resistances in limit analysis of hemispherical masonry domes, Frattura ed Integrità Strutturale, 14 (2020) 336-355.

[8] C. Casapulla, E. Mousavian, M. Zarghani, A digital tool to design structurally feasible semi-circular masonry arches composed of interlocking blocks, Computers & Structures, 221 (2019) 111-126.

[9] P. Roca, M. Cervera, L. Pelà, R. Clemente, M. Chiumenti, Continuum FE models for the analysis of Mallorca Cathedral, Engineering Structures, 46 (2013) 653-670.

[10] D.V. de Castro Oliveira, Experimental and numerical analysis of blocky masonry structures under cyclic loading, in, Universidade do Minho, 2003.

[11] P.B. Lourenco, Computational strategies for masonry structures, in, TU Delft, The Netherlands, The Netherlands, 1996.

[12] J. McInerney, M.J. DeJong, Discrete Element Modeling of Groin Vault Displacement Capacity, International Journal of Architectural Heritage, 9 (2015) 1037-1049.

[13] T.E. Boothby, Analysis of masonry arches and vaults, Progress in Structural Engineering and Materials, 3 (2001) 246-256.

[14] G. Angjeliu, G. Cardani, D. Coronelli, Digital Modelling and Analysis of Masonry Vaults, ISPRS - International Archives of the Photogrammetry, Remote Sensing and Spatial Information Sciences, XLII-2/W11 (2019) 83-89.

[15] B. Riveiro, P. Morer, P. Arias, I. de Arteaga, Terrestrial laser scanning and limit analysis of masonry arch bridges, Construction and Building Materials, 25 (2011) 1726-1735.

[16] L. Binda, Learning from failure: long-term behaviour of heavy masonry structures, WIT press, 2008.

[17] R. Barthel, Crack Formation in Masonry Cross Vaults, IABSE Reports, (1993) 393-400.

[18] D. D'Ayala, E. Speranza, Definition of collapse mechanisms and seismic vulnerability of historic masonry buildings, Earthquake Spectra, 19 (2003) 479-509.

[19] G. Bartoli, M. Betti, C. Borri, Numerical Modeling of the Structural Behavior of Brunelleschi's Dome of Santa Maria del Fiore, International Journal of Architectural Heritage, 9 (2015) 408-429.

[20] K.G. Talley, J. Arrellaga, J.E. Breen, Computational Modeling of Existing Damage in Concrete Bridge Columns, Journal of Structural Engineering, 140 (2014) 06014006.

[21] G. Angjeliu, G. Cardani, D. Coronelli, A parametric model for ribbed masonry vaults, Automation in Construction, 105 (2019) 102785.

[22] G. Angjeliu, D. Coronelli, G. Cardani, Numerical Analysis of Mechanical Damage in Ribbed Masonry Vaults under Differential Settlements, International Journal of Architectural Heritage, (2021) 1-18.

[23] G. Lengyel, K. Bagi, Numerical analysis of the mechanical role of the ribs in groin vaults, Computers & Structures, 158 (2015) 42-60.

[24] E. Bertolesi, J.M. Adam, P. Rinaudo, P.A. Calderón, Research and practice on masonry cross vaults – A review, Engineering Structures, 180 (2019) 67-88.

[25] A. Gaetani, G. Monti, P.B. Lourenço, G. Marcari, Design and Analysis of Cross Vaults Along History, International Journal of Architectural Heritage, 10 (2016) 841-856.

[26] G. Cardani, G. Angjeliu, Integrated Use of Measurements for the Structural Diagnosis in Historical Vaulted Buildings, Sensors, 20 (2020) 4290.

[27] G.A. Breymann, Allgemeine Bau-Constructions-Lehre, mit besonderer Beziehung auf das Hochbauwesen: Ein Leitfaden zu Vorlesungen und zum Selbstunterrichte, Hoffmann, 1849.

[28] E.-E. Viollet-le-Duc, Dictionnaire raisonné de l'architecture française du XIe au XVIe siècle, 10 vols., Morel, Paris, 1854 -1868.

[29] A. Choisy, Histoire de l'architecture, Rouveyre, 1899.

[30] A.K. Porter, The construction of Lombard and Gothic vaults, Elliots Books, 1911.

[31] J. Fitchen, The construction of Gothic cathedrals: a study of medieval vault erection, University of Chicago Press, 1981.

[32] D. Theodossopoulos, B.P. Sinha, Function and technology of historic cross vaults, Progress in Structural Engineering and Materials, 6 (2004) 10-20.

[33] C. Ferrari da Passano, Il Duomo rinato: Storia e tecnica del restauro statico dei piloni del tiburio del Duomo di Milano [in Italian], Veneranda Fabbrica del Duomo (Diakronia), Milan, 1988.

[34] A. Croce, Antichi monumenti e città. Ricerca e conservazione. An overview., Geotechnical Engineering in Italy, (1985) 57-110.

[35] D. Coronelli, C. di Prisco, F. Pisanò, S. Imposimato, S. Ghezzi, M. Pesconi, The tiburio of the cathedral of Milan: Structural analysis of the construction & 20th century foundation settlements, (2014).

[36] D. Coronelli, B. Caggioni, F. Zanella, The Cathedral of Milan: the structural history of the load-bearing system, International Journal of Architectural Heritage, (2015).

[37] G. Cardani, D. Coronelli, G. Angjeliu, Damage observation and settlement mechanisms in the naves of the Cathedral of Milan, in: Structural Analysis of Historical Constructions (SAHC) Leuven, Belgium, 2016.

[38] M. Vasic, A multidisciplinary approach for the structural assessment of historical constructions with tie-rods, in, 2015.

[39] G. Angjeliu, D. Coronelli, G. Cardani, T. Boothby, Structural assessment of iron tie rods based on numerical modelling and experimental observations in Milan Cathedral, Engineering Structures, 206 (2020) 109690.

[40] G. Angjeliu, D. Coronelli, G. Cardani, Development of the simulation model for Digital Twin applications in historical masonry buildings: the integration between numerical and experimental reality, Computers & Structures, (2020).

[41] VFD, Annali della fabbrica del duomo di Milano, dall'origine fino al presente, Milano, 1877 - 1885.

[42] A.M. D'Altri, S. De Miranda, G. Castellazzi, V. Sarhosis, J. Hudson, D. Theodossopoulos, Historic Barrel Vaults Undergoing Differential Settlements, International Journal of Architectural Heritage, (2019) 1-14.

[43] J. Lubliner, J. Oliver, S. Oller, E. Onate, A Plastic-Damage Model for Concrete, International Journal of Solids and Structures, 25 (1989) 299-326.

[44] D. Hibbitt, B. Karlsson, P. Sorensen, ABAQUS Manual, Dassault Systèmes, Providence, RI, USA, 2016.

[45] P. Condoleo, A. Gobbo, A. Taliercio, A Hybrid Masonry and Steel Mirror-Type Vault with Lunettes: Survey and Structural Analysis, International Journal of Architectural Heritage, 14 (2020) 496-516.

[46] M. Bruggi, A. Taliercio, Nonlinear behaviour and macroscopic strength of Flemish bond masonry, International Journal of Masonry Research and Innovation, 7 (2022) 126-145.

[47] G. Angjeliu, Integrated structural modelling and experimental observations in historic masonry constructions, in: PhD Thesis, Department of Civil and Environmental Engineering, Politecnico di Milano, Milan (IT), Politecnico di Milano, 2018, pp. 312.

[48] M. Como, Statics of Historic Masonry Constructions, in, Springer, 2015.